



## Performance and Cost Comparison of Building Structures with SRPM and Shearwall in Seismic Dynamic Analysis

Difla Yustisiya Qur'ani<sup>1</sup>, Roro Sulaksitaningrum<sup>1</sup>

<sup>1</sup>Civil Engineering, State University of Malang, Malang, Indonesia

\*Corresponding Author: Difla Yustisiya Qur'ani

Email: [difla.yustisiya.2105236@students.um.ac.id](mailto:difla.yustisiya.2105236@students.um.ac.id)



### Article Info

#### Article history:

Received 27 February 2025

Received in revised form 3

May 2025

Accepted 12 May 2025

#### Keywords:

Earthquake-Resistant Design

Shearwall

SRPM

Structural Analysis

Cost Efficiency

### Abstract

*As a country located on the Pacific Ring of Fire, Indonesia faces a high seismic risk, necessitating the design of earthquake-resistant buildings. This study evaluates the seismic performance and cost implications of multi-story U-shaped buildings using the Moment Resisting Frame System (SRPM) and shear walls. Four structural models with different configurations were analyzed using ETABS 22 for structural behavior and Microsoft Excel for cost estimation. The results indicate that models with shear walls exhibit better lateral stiffness, resulting in shorter fundamental periods and smaller interstory drifts. Model 2 demonstrated the best seismic resistance, making it the primary choice for earthquake-prone areas. However, the cost analysis showed that models without shear walls, particularly Model 4, were more economical. While shear walls increase initial construction costs, they offer long-term benefits by reducing potential structural damage and post-earthquake maintenance costs. This study provides valuable insights into balancing seismic safety and cost efficiency, assisting in the selection of the optimal structural system for earthquake-prone regions.*

## Introduction

Earthquakes are one of the most destructive natural disasters, potentially causing severe damage to buildings and infrastructure, especially in regions located within active seismic zones. Indonesia, situated along the Pacific Ring of Fire, faces a high seismic risk, including Malang City, which is located in the southern part of Java Island (Nofirman et al., 2023). Therefore, designing and constructing earthquake-resistant buildings is crucial to minimizing damage and casualties.

U-shaped buildings are commonly chosen in urban areas as they maximize land usage while allowing for open spaces that serve various functions, such as courtyards or public areas. However, U-shaped structures are more vulnerable to strong lateral forces generated by earthquakes, increasing the risk of structural damage. According to Kartiko et al. (2021) buildings with irregular floor plans, such as U-, L-, or T-shaped layouts, exhibit inferior seismic behavior compared to those with simple regular floor plans (Kartiko et al., 2021). Therefore, an effective lateral load-resisting system is required to enhance the seismic resistance of such structures.

One of the most commonly used methods to improve the seismic performance of multi-story buildings is the implementation of the Moment Resisting Frame System (SRPM) and shear walls (Wibowo & Zebua, 2021). These systems are effective in controlling lateral displacement and reducing shear forces within the structure (Maghribi et al., 2022). SRPM is designed to resist lateral loads through flexural action in its structural elements, while shear

walls provide resistance through their inherent stiffness and shear strength (Khairudin & Ryanto, 2023). This study aims to compare the seismic performance and construction costs of U-shaped multi-story buildings using SRPM and shear walls in Malang City. By analyzing these two structural systems, this research seeks to provide a safer and more cost-effective solution for earthquake-prone regions.

The fundamental period of a structure is the time required for a structure to complete one full cycle of vibration when displaced from its equilibrium position and returning to its initial state (Wijayanti, 2017). This period reflects the natural dynamic characteristics of the structure and is crucial in earthquake-resistant building design, as it influences the structural response to seismic loads (Mustika et al., 2022). Generally, the fundamental period ( $T$ ) is influenced by the mass and stiffness of the structure. Structures with larger mass or lower stiffness tend to have longer fundamental periods, while those with smaller mass or higher stiffness exhibit shorter periods. The fundamental period is calculated using the following equation:

$$T = C_u \times T_a \quad (1)$$

Where:

$C_u$  = Upper-bound Period Coefficient

$T_a$  = Approximate Fundamental Period

For preliminary design, empirical formulas that consider the structural system type and building height are used to estimate the fundamental period. According to SNI 1726:2019 (Sistem & Standar, 2020), the approximate fundamental period ( $T_a$ ) can be calculated using the equation:

$$T_a = C_t \times h^x \quad (2)$$

Where:

$C_t$  = Approximate Period Parameter (SNI)

$x$  = Approximate Period Parameter (SNI)

$h$  = Building Height

Seismic shear force refers to the horizontal forces exerted at the base of a structure due to seismic activity, such as earthquakes. These forces arise from ground acceleration, which induces inertia forces in the building mass, causing lateral loads on the structure. Seismic shear force is a critical parameter in earthquake-resistant building design to ensure structural stability and safety (Saputro & Rahayu, 2021). In general, the seismic base shear force can be calculated using the following equation:

$$T_a = C_s \times W \quad (3)$$

Where:

$C_s$  = Seismic Response Coefficient of the Structure

$W$  = Total Building Weight

The seismic response coefficient is determined based on factors such as gravitational acceleration, structural response modification factor, and the seismic characteristics of the site location (Wisena, 2018).

Interstory drift is the relative lateral displacement between two consecutive floors of a building due to lateral loads such as earthquakes or wind forces (Hasan & Astira, 2013). This parameter is essential in structural design as it relates to the deformation experienced by non-structural components such as partition walls, facades, and architectural elements, impacting occupant comfort and building integrity. According to SNI 1726:2019 (Sistem & Standar, 2020), the interstory drift limit is determined using the following equation:

$$\theta = \frac{\Delta}{h} \leq \theta_{maks} \quad (4)$$

Where:

$\theta$  = Interstory drift ratio

$h$  = Story height

$\theta_{maks}$  = Maximum allowable limit

The P-Delta effect is a structural engineering phenomenon describing the impact of axial loads (P) on lateral displacements ( $\Delta$ ) in a structure (Suranto et al., 2024). When a structure experiences lateral displacement due to loads such as wind or earthquakes, the axial load applied to the structure generates secondary moments, potentially increasing deformation and internal forces. This effect is crucial in structural analysis and design, as it affects overall building stability and performance. The P-Delta effect is calculated using the equation:

$$\theta = \frac{P_x \Delta l_e}{V_x h_{xx} C_d} \quad (5)$$

Where:

$\theta$  = Stability Coefficient

$P_x$  = Total vertical design load at, and above the x-level

$\Delta$  = Deviation between design levels

$l_e$  = Earthquake primacy factor

$V_x$  = Seismic shear force acting between levels x and x-1

$h_{xx}$  = Height below x level

$C_d$  = Deflection magnification factor

In calculating the P-Delta Effect, the stability coefficient should not exceed  $\theta_{max}$  which is determined as follows:

$$\theta_{max} = \frac{0,5}{\beta C_d} \leq 0,25 \quad (6)$$

Where:

$\beta$  = The ratio of shear demand to shear capacity, this ratio is permitted to be conservatively taken as 1.0.

If the stability coefficient ( $\theta$ ) is greater than 0.1 but less than or equal to  $\theta_{max}$ , the enhancement factor related to the P-Delta Effect on the displacements and forces of the structural components should be determined by rational analysis. Alternatively, it is permitted to multiply the displacement and force of the structure by  $1.0/(1-\theta)$ . If  $\theta$  is greater than  $\theta_{max}$ , then the structure is potentially unstable (Sistem & Standar, 2020).

Cost Estimation is a detailed estimate of the total costs required to complete a project, including material costs, labor wages, equipment, and other expenses associated with project execution. Cost Estimation serves as a planning and cost control tool in construction projects, ensuring that the project can be completed within the allocated budget (Atssauri, 2016). The preparation of the Cost Estimation is generally based on planning documents that include technical drawings, job specifications, and work volume lists. The accuracy of Cost Estimation preparation depends on the precision of the data used, such as material prices, labor productivity standards, and project implementation methods (Abidin, 2021). In this study, the cost estimation of the Project Budget Plan focuses on the cost parameters of structural elements. The cost estimation is based on the Unit Price Analysis (AHSP) as stipulated in the "Peraturan Walikota Malang Nomor 10 Tahun 2022" concerning Unit Prices of Construction Work in Malang City (Malang, 2022). This budget calculation is used as a cost comparison to determine the most efficient among the four models analyzed.

## Methods

This research analyzes four U-shaped reinforced concrete building models, each five stories high with a floors height of 4.5 meters. Columns, beams, and floor slabs are made of concrete with a compressive strength ( $f_c'$ ) of 28 MPa, and all floor slabs have a thickness of 140 mm. The buildings are designed as educational facilities in Malang City, classified under Seismic Design Category (SDC) D, with medium soil conditions. The primary variation among the models involves beam dimensions and the structural system (SRPM or shear walls). Structural performance analysis was conducted using ETABS 22, while cost analysis was performed using Microsoft Excel. The research methodology follows the flowchart shown in Figure 1.

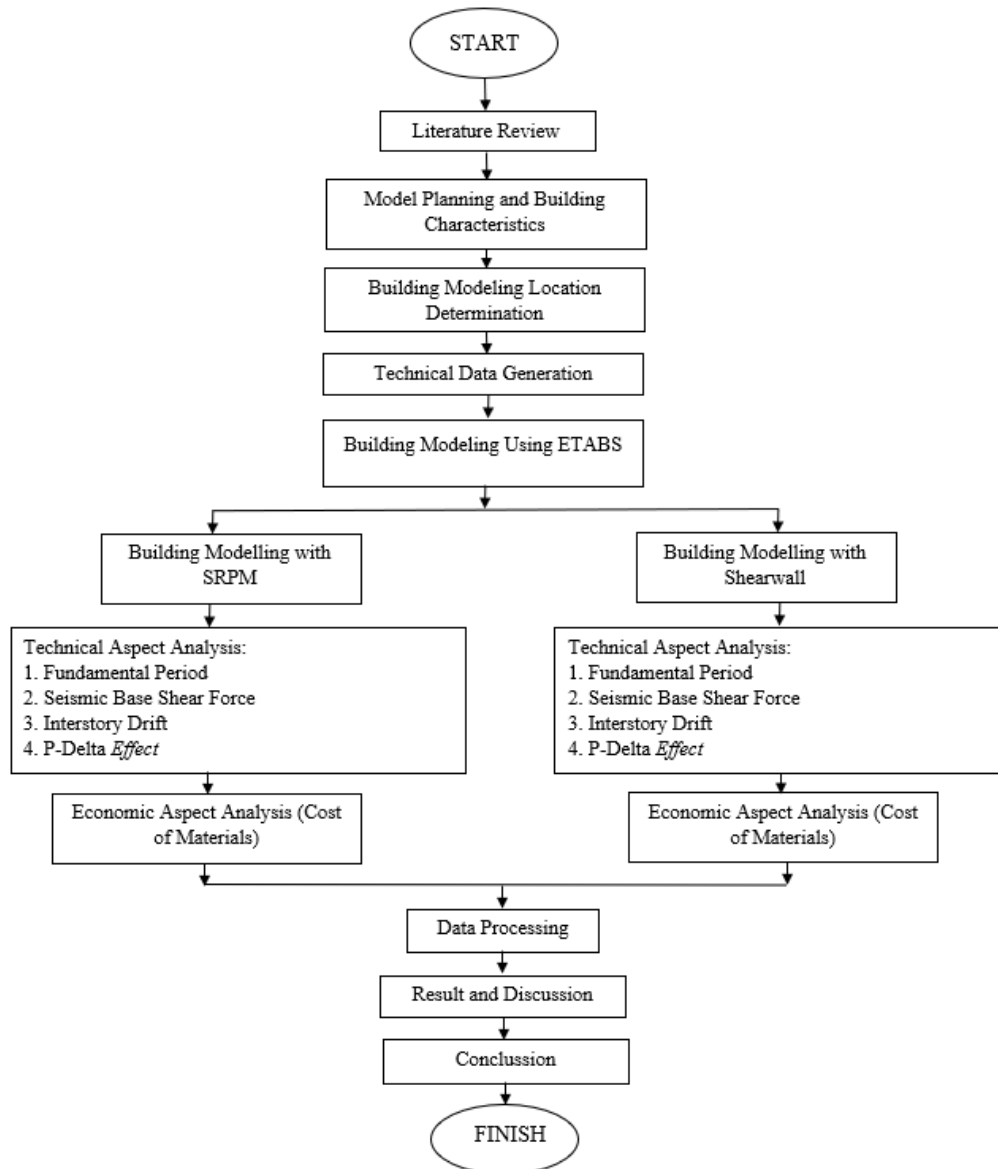


Figure 1. Research Flowchart

Table 1-4 summarize the structural component dimensions for each model, and Table 5 describes the structural variations.

Table 1. Structure Design Summary of Model 1

MODEL 1	Story	Dimensions
K1 Column	1-5	450 x 450 mm
B1 Beam	1-5	650 x 325 mm
B2 Beam	1-5	500 x 250 mm

Floor Slab	1-5	140 mm
Shearwall	1-5	6000 x 250 mm

Table 2. Structure Design Summary of Model 2

<b>MODEL 2</b>	<b>Story</b>	<b>Dimensions</b>
K1 Column	1-5	450 x 450 mm
B1 Beam	1-5	625 x 312,5 mm
B2 Beam	1-5	475 x 237,5 mm
Floor Slab	1-5	140 mm
Shearwall	1-5	6000 x 250 mm

Table 3. Structure Design Summary of Model 3

<b>MODEL 3</b>	<b>Story</b>	<b>Dimensions</b>
K1 Column	1-5	450 x 450 mm
B1 Beam	1-5	625 x 325 mm
B2 Beam	1-5	500 x 250 mm
Floor Slab	1-5	140 mm
Shearwall	1-5	None

Table 4. Structure Design Summary of Model 4

<b>MODEL 4</b>	<b>Story</b>	<b>Dimensions</b>
K1 Column	1-5	450 x 450 mm
B1 Beam	1-5	625 x 312,5 mm
B2 Beam	1-5	475 x 237,5 mm
Floor Slab	1-5	140 mm
Shearwall	1-5	None

The variations in each analyzed model are detailed in Table 5. B2 Beam was chosen for variation as it plays a crucial role in distributing lateral forces caused by earthquakes. This is because changes in the dimensions of structural elements, especially linking beams, can influence resistance to lateral deformation (Zhao & Dong, 2020).

Table 5. Model Variation

<b>MODEL</b>	<b>B2 Beam</b>	<b>Structure System</b>
Model 1	500 x 250 mm	<i>Shearwall</i>
Model 2	475 x 237,5 mm	<i>Shearwall</i>
Model 3	500 x 250 mm	SRPM
Model 4	475 x 237,5 mm	SRPM

The construction cost data for structural implementation is based on the Unit Price Analysis (AHSP) as stipulated in the “Peraturan Walikota Malang Nomor 10 Tahun 2022” concerning Unit Prices of Construction Work in Malang City (Malang, 2022), as presented in Table 6.

Table 6. Unit Price of Work

<b>No.</b>	<b>Work Items</b>	<b>Unit Price (m<sup>3</sup>)</b>
1	Structural Work of K-350 reinforced concrete beam	Rp. 10.435.616,00
2	Structural Work of K-350 reinforced concrete column	Rp. 12.198.019,00
3	Structural Work of K-350 reinforced concrete wall	Rp. 10.435.616,00
4	Structural Work of K-350 reinforced concrete floor slab	Rp. 9.325.733,00

The typical floor plan of the building is presented in Figure 2. The 3D model of shear wall placement in Model 1 and Model 2 is positioned identically and assumed to be present on all

floors, as shown in Figure 3. The 3D model of the structure using the Moment Resisting Frame System (SRPM) for Model 3 and Model 4 is displayed in Figure 4.

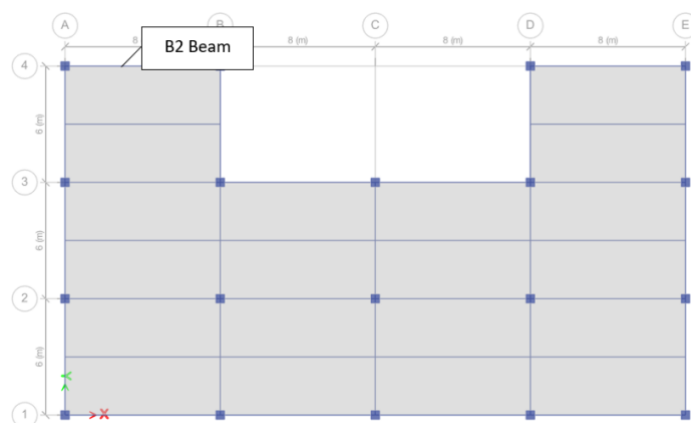


Figure 2. Typical Floor Plan

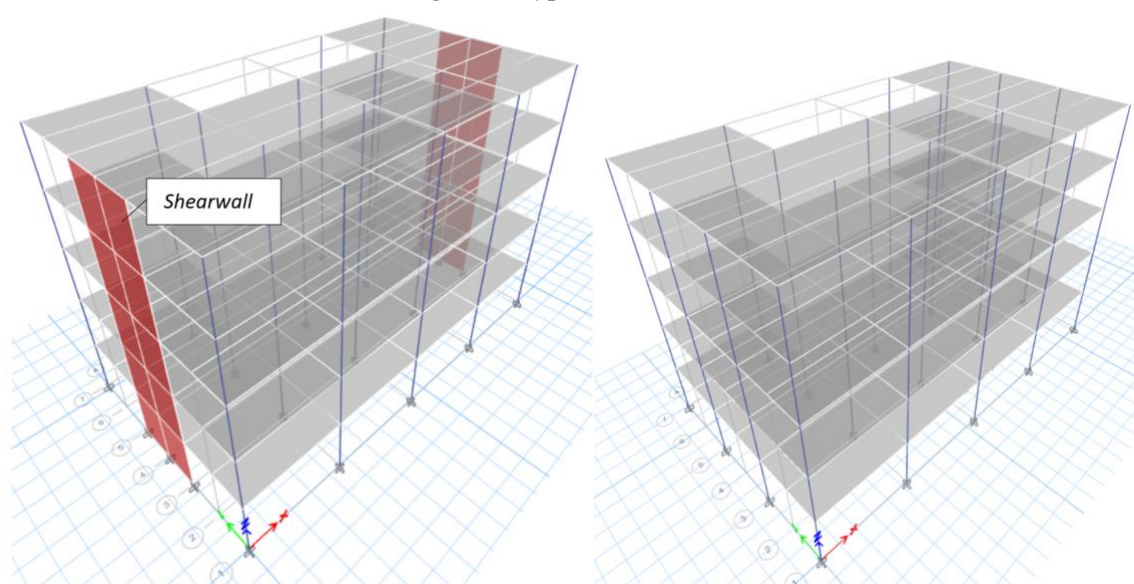


Figure 3. 3D Model of Structure with Shearwall    Figure 4. 3D Model of Structure with SRPM

## Results and Discussion

### Structure Fundamental Period

The fundamental period of the structure was calculated using the ETABS application and is detailed in Table 7. The output from the ETABS analysis is recorded in the "Resulting Period" column, while the fundamental period used in the analysis is listed in the "Wear Period" column. The wear period is the smaller value between the ETABS analysis output and the maximum period calculated using Equation (1).

Based on the ETABS analysis results presented in Table 7, Model 1 and Model 2 exhibit smaller fundamental period values compared to Model 3 and Model 4. This indicates the implementation of shear walls in Models 1 and 2 enhances structural stiffness, thereby reducing the fundamental period (Fares, 2019).

Table 7. Structure Fundamental Period

	Resulting Period (s)	Wear Period (s)
<b>MODEL 1</b>		
X direction	0,8354	0,7058
Y direction	0,7013	0,1013

<b>MODEL 2</b>		
X direction	0,8386	0,7058
Y direction	0,7054	0,7054
<b>MODEL 3</b>		
X direction	0,8297	0,8297
Y direction	0,8351	0,8351
<b>MODEL 4</b>		
X direction	0,758	0,758
Y direction	0,8314	0,8314

Model 2 is the most recommended model for high-seismic-risk conditions due to its shorter fundamental period. A shorter fundamental period helps reduce the potential for resonance during an earthquake (Zhao & Dong, 2020).

### Seismic Shear Force

Seismic shear force was analyzed using two calculation methods: manual calculations and ETABS output. The manual calculation was performed using Equation (3). The analysis results are presented in Table 8.

Table 8. Seismic Base Shear Force

	<b>Manual (kN)</b>	<b>ETABS (kN)</b>
<b>MODEL 1</b>		
X direction	3582,2	3582,19
Y direction	3582,2	3582,19
<b>MODEL 2</b>		
X direction	1902,23	1902,23
Y direction	1902,23	1902,23
<b>MODEL 3</b>		
X direction	1662,37	1662,42
Y direction	1662,37	1662,42
<b>MODEL 4</b>		
X direction	1557,44	1557,44
Y direction	1557,44	1557,44

As shown in Table 8, Model 1 has the highest base shear force due to its greater structural stiffness resulting from the use of shear walls. In contrast, Model 4 has the lowest shear force because it does not incorporate shear walls and features the smallest beam cross-section. According to a study by Hidayat et al. (2020), structures with shear walls tend to have a higher shear force distribution but are more effective in reducing lateral deformation (Pierre & Hidayat, 2020).

### Interstory Drift

To determine the interstory drift, displacement data obtained from ETABS is required. The displacement data in both the x and y directions is processed to generate the Inelastic Drift values, as shown in Tables 9 to 12. The interstory drift is considered safe (indicated as "OK") if it meets the criteria defined by Equation (4).

Table 9. Interstory Drift of Model 1

<b>MODEL 1</b>	<b><math>\Delta x</math> (mm)</b>	<b><math>\Delta y</math> (mm)</b>	<b>Drift Limit (mm)</b>	<b>Status</b>
5 <sup>th</sup> floor	50,05	33,16	90,00	OK
4 <sup>th</sup> floor	76,48	31,99	90,00	OK
3 <sup>rd</sup> floor	102,11	28,07	90,00	NOT OK

2 <sup>nd</sup> floor	122,52	20,52	90,00	NOT OK
1 <sup>st</sup> floor	92,61	8,72	90,00	NOT OK

Table 10. Interstory Drift of Model 2

MODEL 2	$\Delta x$ (mm)	$\Delta y$ (mm)	Drift Limit (mm)	Status
5 <sup>th</sup> floor	16,45	10,51	90,00	OK
4 <sup>th</sup> floor	29,53	10,38	90,00	OK
3 <sup>rd</sup> floor	40,73	9,32	90,00	OK
2 <sup>nd</sup> floor	47,51	7,02	90,00	OK
1 <sup>st</sup> floor	35,09	3,25	90,00	OK

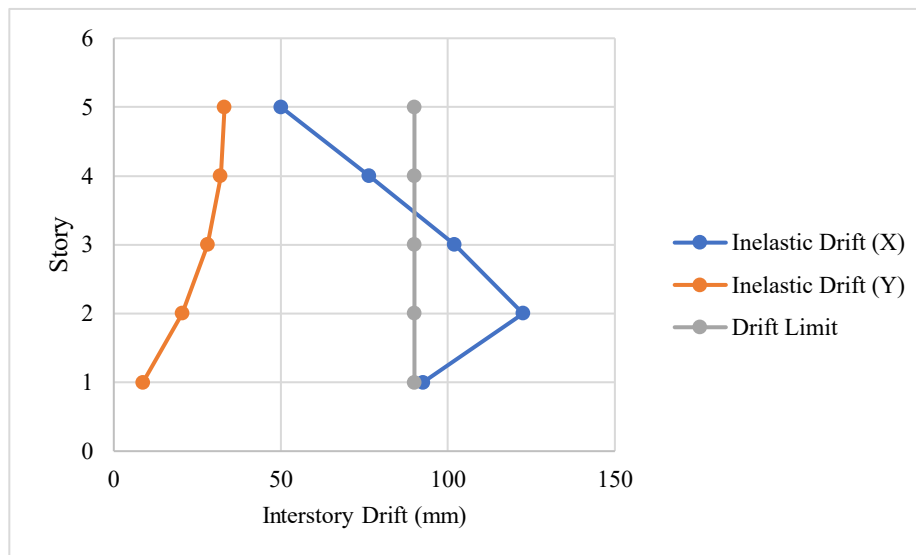


Figure 5. Model 1 Interstory Drift Graph

Table 11. Interstory Drift of Model 3

MODEL 3	$\Delta x$ (mm)	$\Delta y$ (mm)	Drift Limit (mm)	Status
5 <sup>th</sup> floor	16,19	19,25	69,23	OK
4 <sup>th</sup> floor	29,87	34,39	69,23	OK
3 <sup>rd</sup> floor	41,42	47,17	69,23	OK
2 <sup>nd</sup> floor	48,81	54,61	69,23	OK
1 <sup>st</sup> floor	38,21	39,64	69,23	OK

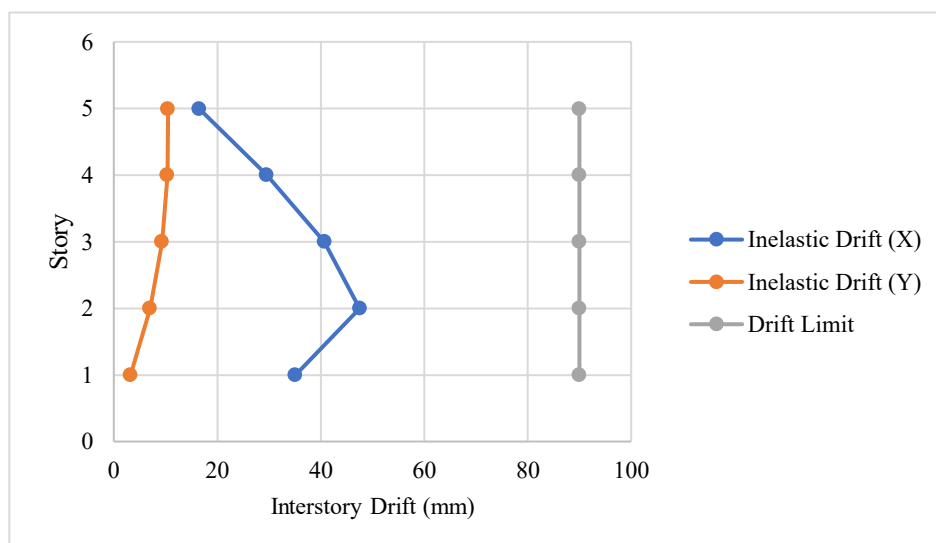


Figure 6. Model 2 Interstory Drift Graph



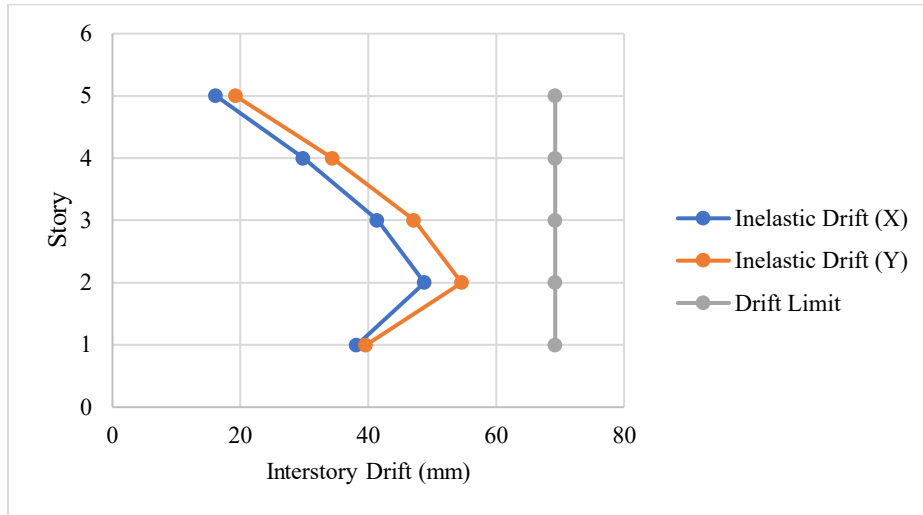


Figure 7. Model 3 Interstory Drift Graph

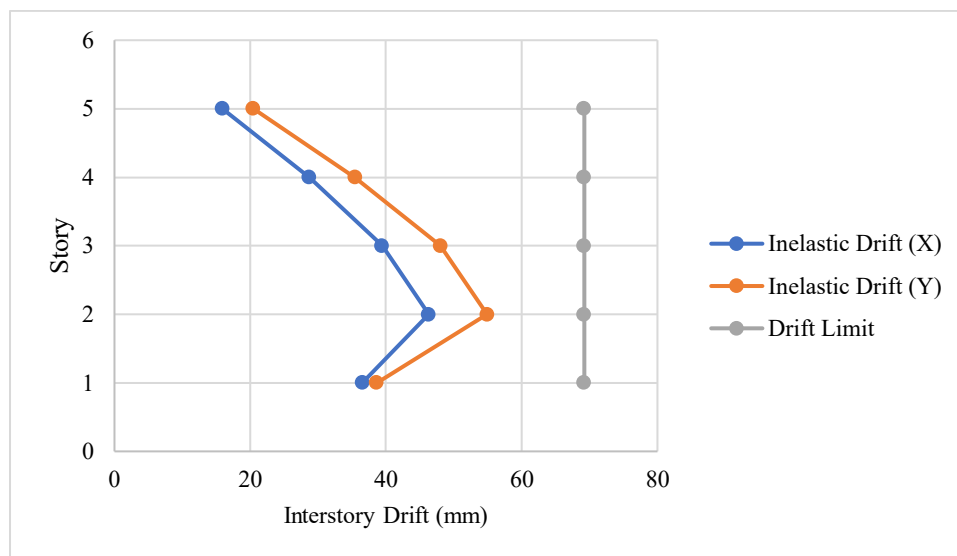


Figure 8. Model 4 Interstory Drift Graph

Table 12. Intestory Drift of Model 4

MODEL 4	$\Delta x=$ (mm)	$\Delta y$ (mm)	Drift Limit (mm)	Status
5 <sup>th</sup> floor	15,91	20,48	69,23	OK
4 <sup>th</sup> floor	28,73	35,46	69,23	OK
3 <sup>rd</sup> floor	39,44	48,03	69,23	OK
2 <sup>nd</sup> floor	46,31	54,91	69,23	OK
1 <sup>st</sup> floor	36,53	38,65	69,23	OK

Notes:  $\Delta x$  = Inelastik Drift x Direction.  $\Delta y$  = Inelastik Drift y Direction

Tables 9 to 12 present the interstory drift for the four tested models. Model 1 shows that several floors do not meet the allowable drift limits, particularly on 2<sup>nd</sup> and 3<sup>rd</sup> floors. In contrast, Models 2, 3, and 4 comply with all permitted drift limits. Exceeding the allowable drift limit can lead to the failure of core structural elements during an earthquake (Çolak et al., 2023). The interstory drift graphs are illustrated in Figures 5 to 8.

### P-Delta Effect

The P-Delta effect analysis is derived from the Inelastic Drift data obtained from the interstory drift calculations in the previous section. This data is further analyzed alongside the Story

Forces data obtained from the ETABS analysis output. The results are presented in Tables 13 to 16 and illustrated in Figures 9 to 12. A structure is considered safe (indicated as "OK") based on the criteria defined by Equation (6).

Table 13. P-Delta Effect of Model 1

MODEL 1	$\theta_x$	$\theta_y$	P Delta Limit	$\theta_{max}$	Status
5 <sup>th</sup> floor	0,035	0,0074	0,1	0,909	OK
4 <sup>th</sup> floor	0,084	0,0098	0,1	0,909	OK
3 <sup>rd</sup> floor	0,142	0,0106	0,1	0,909	NOT OK
2 <sup>nd</sup> floor	0,201	0,0092	0,1	0,909	NOT OK
1 <sup>st</sup> floor	0,168	0,0047	0,1	0,909	NOT OK

Table 14. P-Delta Effect of Model 2

MODEL 2	$\theta_x$	$\theta_y$	P Delta Limit	$\theta_{max}$	Status
5 <sup>th</sup> floor	0,006	0.002	0,1	0,909	OK
4 <sup>th</sup> floor	0,014	0.003	0,1	0,909	OK
3 <sup>rd</sup> floor	0,024	0,003	0,1	0,909	OK
2 <sup>nd</sup> floor	0,032	0,003	0,1	0,909	OK
1 <sup>st</sup> floor	0,028	0,002	0,1	0,909	OK

Table 15. P-Delta Effect of Model 3

MODEL 3	$\theta_x$	$\theta_y$	P Delta Limit	$\theta_{max}$	Status
5 <sup>th</sup> floor	0,005	0.006	0,1	0,909	OK
4 <sup>th</sup> floor	0,013	0.014	0,1	0,909	OK
3 <sup>rd</sup> floor	0,021	0,024	0,1	0,909	OK
2 <sup>nd</sup> floor	0,029	0,032	0,1	0,909	OK
1 <sup>st</sup> floor	0,026	0,027	0,1	0,909	OK

Table 16. P-Delta Effect of Model 4

MODEL 4	$\theta_x$	$\theta_y$	P Delta Limit	$\theta_{max}$	Status
5 <sup>th</sup> floor	0,006	0.008	0,1	0,909	OK
4 <sup>th</sup> floor	0,016	0.022	0,1	0,909	OK
3 <sup>rd</sup> floor	0,027	0,036	0,1	0,909	OK
2 <sup>nd</sup> floor	0,037	0,049	0,1	0,909	OK
1 <sup>st</sup> floor	0,034	0,039	0,1	0,909	OK

Notes:  $\theta_x$  = Stability Coefficient in x direction  $\theta_y$  = Stability Coefficient in y direction  $\theta_{max}$  = Stability Limit of the Structure

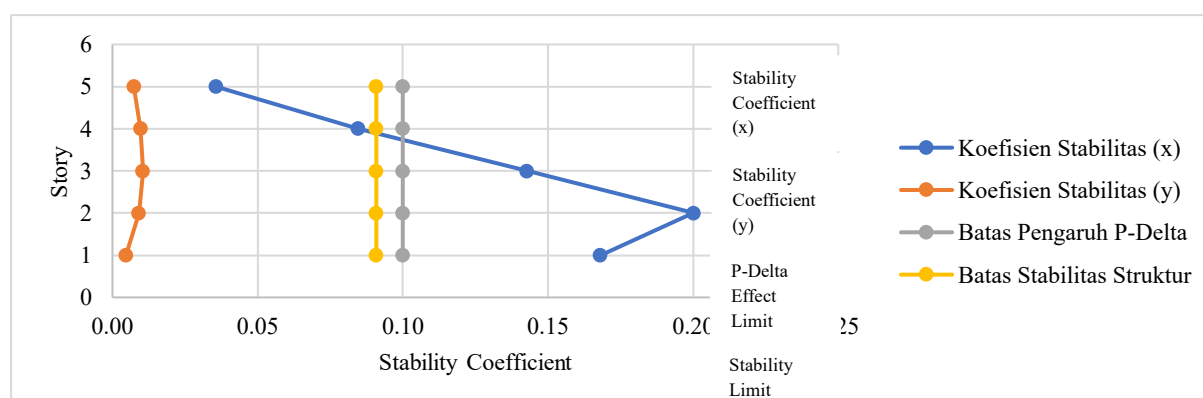


Figure 9. Model 1 P-Delta Effect Graph

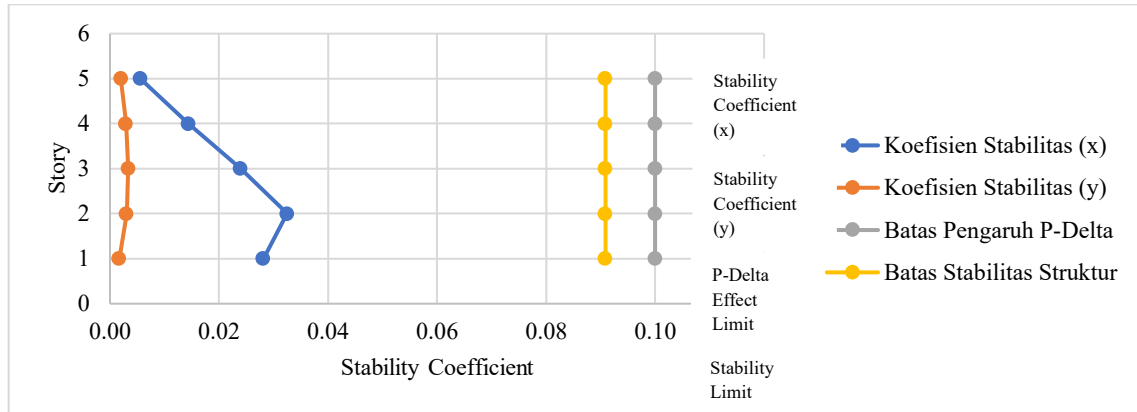


Figure 10. Model 2 P-Delta Effect Graph

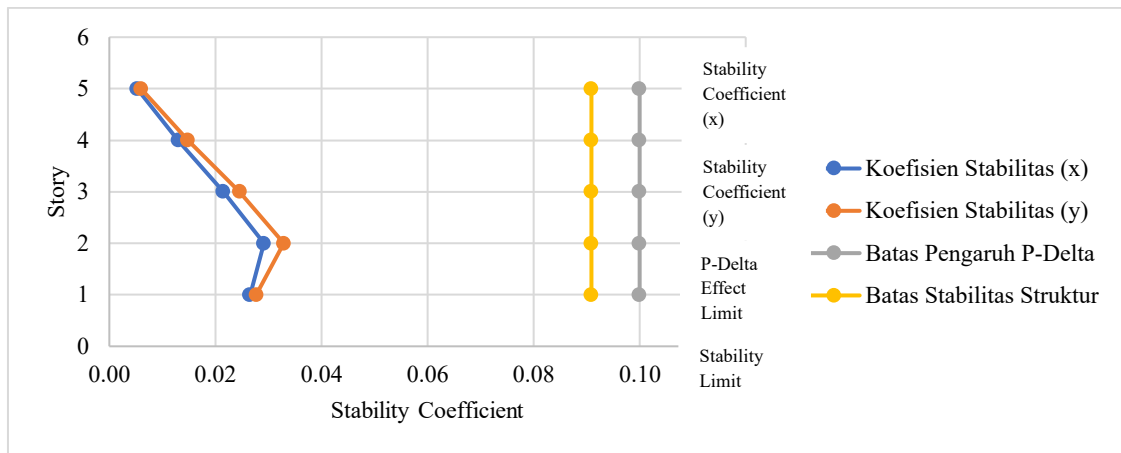


Figure 11. Model 3 P-Delta Effect Graph

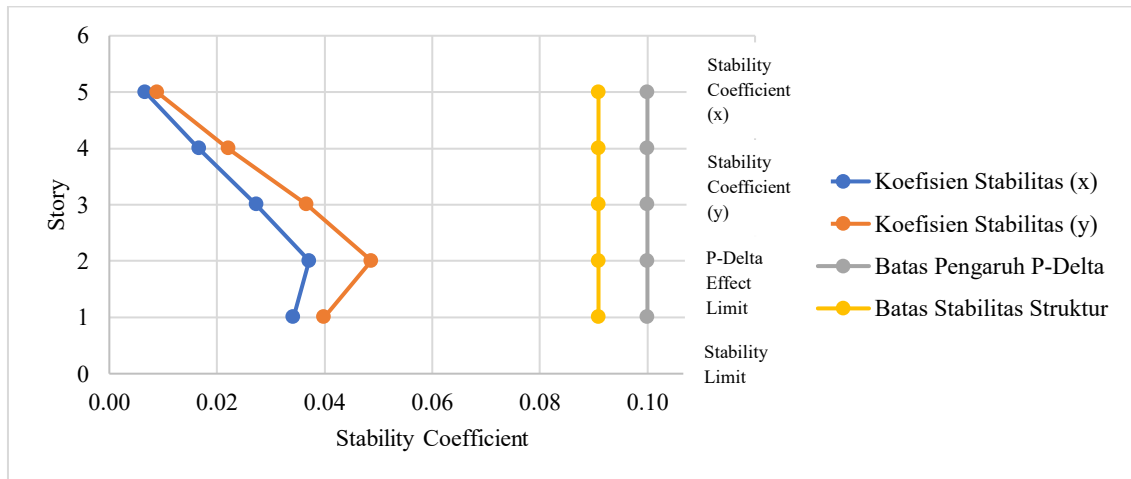


Figure 12. Model 4 P-Delta Effect Graph

The P-Delta effect calculations presented in Tables 13 to 16 indicate that Model 1 has a stability coefficient exceeding the allowable limit on several floors, particularly on the lower levels. In contrast, Models 2, 3, and 4 remain within safe limits. Excessive P-Delta effects can lead to structural instability and increase the risk of progressive collapse (Siregar et al., 2024). Therefore, Model 1 requires design optimization to mitigate this effect, such as enhancing the capacity of structural elements on the lower floors.

### Cost Estimation

The cost estimation in this study refers to the Unit Price Analysis (AHSP) as regulated by the “Peraturan Walikota Malang Nomor 10 Tahun 2022” on Unit Prices of Construction Work in

Malang City (Malang, 2022). The budget plan focuses on the costs of structural element works according to the analyzed models. The detailed budget plan is presented in Tables 17 to 20.

Table 17. Model 1 Cost Estimation Table

<b>MODEL 1</b>	<b>Cost</b>
Type 1 Beam Work	Rp. 2.327.977.217,00
Type 2 Beam Work	Rp. 563.523.264,00
Column Work	Rp. 1.055.967.257,00
Floor Slab Work	Rp. 3.506.366.976,00
Shearwall Work	Rp. 629.486.977,50
<b>TOTAL</b>	Rp. 8.083.321.692,00

Table 18. Model 2 Cost Estimation Table

<b>MODEL 2</b>	<b>Cost</b>
Type 1 Beam Work	Rp. 2.152.345.800,00
Type 2 Beam Work	Rp. 508.579.745,80
Column Work	Rp. 1.055.967.257,00
Floor Slab Work	Rp. 3.506.366.976,00
Shearwall Work	Rp. 629.486.977,50
<b>TOTAL</b>	Rp. 7.852.746.757,00

Table 19. Model 3 Cost Estimation Table

<b>MODEL 3</b>	<b>Cost</b>
Type 1 Beam Work	Rp. 2.539.611.510,00
Type 2 Beam Work	Rp. 657.443.808,00
Column Work	Rp. 1.055.967.257,00
Floor Slab Work	Rp. 3.506.366.976,00
Shearwall Work	Rp. 0,00
<b>TOTAL</b>	Rp. 7.759.389.551,00

Table 20. Model 4 Cost Estimation Table

<b>MODEL 4</b>	<b>Cost</b>
Type 1 Beam Work	Rp. 2.348.013.600,00
Type 2 Beam Work	Rp. 593.343.036,00
Column Work	Rp. 1.055.967.257,00
Floor Slab Work	Rp. 3.506.366.976,00
Shearwall Work	Rp. 0,00
<b>TOTAL</b>	Rp. 7.503.690.870,00

Tables 17 to 20 present the cost comparison of the four tested models. Model 1 has the highest cost, followed by Model 2, Model 3, and Model 4. This cost difference is primarily due to the use of shear walls in Models 1 and 2, which increase the demand for reinforced concrete materials. Although shear walls raise initial construction costs, they can reduce maintenance costs in the long run by minimizing potential damage during earthquakes (Putra et al., 2023). Therefore, cost evaluation should consider both structural resilience and the building's life-cycle costs.

## Conclusion

Based on the structural performance analysis and cost estimation of the four U-shaped building models utilizing SRPM and shear walls, the following conclusions were drawn: 1) Models with shear walls (Models 1 and 2) exhibit superior seismic performance compared to

models without shear walls (Models 3 and 4), particularly in reducing fundamental periods and interstory drift; 2) Model 2 demonstrated the best seismic performance, making it the most recommended choice for earthquake-prone areas like Malang City; 3) From a cost perspective, models without shear walls (Models 3 and 4) were more economical, with Model 4 being the least expensive; 4) While shear walls increase initial construction costs, they offer long-term benefits by reducing potential structural damage and post-earthquake repair costs. Selecting the optimal structural system should balance seismic performance and cost efficiency based on project-specific needs. For projects prioritizing earthquake resistance, Model 2 is recommended, whereas Model 4 serves as a cost-efficient alternative with additional reinforcement strategies for seismic resilience.

## References

- Abidin, Khanif Fazal. (2021). *PEMBANGUNAN GEDUNG (Studi Kasus Pembangunan RSUD Ketanggungan Kabupaten Brebes) Disusun dalam Rangka Memenuhi Salah Satu Persyaratan Guna Mencapai Gelar Magister Teknik (MT) Oleh: KHANIF FAZAL ABIDIN NIM : 20201700018 PROGRAM STUDI MAGISTER TEKNIK SIPIL*.
- Atssauri, F. S. (2016). *Analisis anggaran dan realisasi proyek sebagai alat perencanaan dan pengendalian biaya proyek: Studi Pada PT Brantas Abipraya (Persero) Di Jombang*. Retrieved from <http://etheses.uin-malang.ac.id/10500/%0Ahttp://etheses.uin-malang.ac.id/10500/1/12520018.pdf>
- Çolak, Hacer, Türker, Hakan T., & Coşkun, Hilmi. (2023). Accurate Estimation of Inter-Story Drift Ratio in Multistory Framed Buildings Using a Novel Continuous Beam Model. *Applied Sciences (Switzerland)*, 13(13). <https://doi.org/10.3390/app13137819>
- Fares, Anas M. (2019). The Effect of Shear Wall Positions on the Seismic Response of Frame-Wall Structures. *International Journal of Civil and Environmental Engineering*, 13(3), 194–198. Retrieved from <https://www.researchgate.net/publication/340679778>
- Siregar, H., Aswin, M., & Syam, B. (2024). Structural Behavior Analysis of the Beam-Column Connections of Existing Steel Structure Buildings based on Finite Element Modeling-Idea StatiCa. In *E3S Web of Conferences* (Vol. 519, p. 04009). EDP Sciences. <https://doi.org/10.1051/e3sconf/202451904009>
- Hasan, A., & Astira, I. F. (2013). *Analisis perbandingan simpangan lateral bangunan tinggi dengan variasi bentuk dan posisi dinding geser. Studi kasus: Proyek apartemen the royale springhill residences* (Doctoral dissertation, Sriwijaya University).
- Kartiko, A. S., Komara, I., Septiarsilia, Y., Fitria, D. K., Istiono, H., & Pertiwi, D. (2021). Analisis geometri bangunan terhadap kinerja seismik menggunakan *Direct Displacement Based Design Method*. *Jurnal Rekayasa Konstruksi Mekanika Sipil (JRKMS)*, 4(2), 73–84. <https://doi.org/10.54367/jrkms.v4i2.1367>
- Khairudin, M. A., & Ryanto, M. (2023). Analisis struktur gedung berlantai dengan *Shear Wall Tube Type* terhadap beban gempa. *Sistem Infrastruktur Teknik Sipil (SIMTEKS)*, 3(2), 260. <https://doi.org/10.32897/simteks.v3i2.1070>
- Maghribi, M. A. I., Wiswamitra, K. A., & Widodo, J. (2022). Perencanaan Ulang Struktur Gedung Dengan Kombinasi Shear Wall Dan Outrigger System Apartemen Grand Shamaya Surabaya Tower Aubrey. *Siklus: Jurnal Teknik Sipil*, 8(2), 174-182.
- Mustika, R., Putra, R. R., & Fitria, R. (2022). Analysis natural periods of structure using microtremor. *Jurnal Teknik Sipil*, 18(2), 328–342. <https://doi.org/10.28932/jts.v18i2.5027>

- Nofirman, N., Harahap, M. A. K., & Andiani, P. (2023). Studi geomorfologi dan perubahan lanskap dalam konteks perubahan lingkungan di Pulau Jawa. *Jurnal Geosains West Science*, 1(3), 126–133. <https://doi.org/10.58812/jgws.v1i03.718>
- Pierre, A. J., & Hidayat, I. (2020). Seismic performance of reinforced concrete structures with pushover analysis. *IOP Conference Series: Earth and Environmental Science*, 426(1), 012045. <https://doi.org/10.1088/1755-1315/426/1/012045>
- Putra, I., Suardika, I. N., & Setyono, E. Y. (2023). Analisis efisiensi struktur dinding geser (*Shear Wall*) pada bangunan bertingkat ditinjau dari segi biaya (Studi kasus pembangunan shelter kebencanaan Baruna) (Doctoral dissertation, Politeknik Negeri Bali).
- Saputro, D. N., & Rahayu, T. F. (2021). Analisis gaya geser seismik terintegrasi *Building Information Modeling* (BIM) 3D. *Jurnal Keilmuan dan Industri Jasa Konstruksi*, 1(1), 85–95. <http://prosiding.uika-bogor.ac.id/index.php/kijik/article/view/337>
- Suranto, J., Aswin, M., & Nursyamsi, N. (2024). Evaluasi ketentuan keamanan model struktur dan level kinerja dari bangunan beton bertulang eksisting akibat beban gempa. *Action Research Literate*, 8(3), 480–491. <https://doi.org/10.46799/ar1.v8i3.320>
- Wibowo, L. S. B., & Zebua, D. (2021). Analisis pengaruh lokasi dinding geser terhadap pergeseran lateral bangunan bertingkat beton bertulang 5 lantai. *Ge-STRAM: Jurnal Perencanaan dan Rekayasa Sipil*, 4(1), 16–20. <https://doi.org/10.25139/jprs.v4i1.3490>
- Wijayanti, A. (2017). *Analisis umur kelelahan struktur bangunan lepas pantai terpancang akibat pengaruh aging corrosion* (Tugas akhir, Departemen Teknik Kelautan ITS).
- Wisena, F. D. (2018). *Evaluasi kinerja seismik struktur gedung dengan analisis pushover sistem konvensional dan sistem precast* (Skripsi, Universitas Lampung).
- Zhao, Y., & Dong, Y. (2020). Seismic response of reinforced concrete frame-shear wall structure with metal rubber-based damper in coupling beam. *Annales de Chimie: Science des Matériaux*, 44(5), 319–326. <https://doi.org/10.18280/acsm.440503>